VOLUME 118, NUMBER 28
JULY 17, 1996

JOURNAL OF THE AMERICAN CHEMICAL SOCIETY

Solution Structures of *i* to *i* + 3 Cyclized Model Peptides: Building Blocks Mimicking Specific Conformations

Hanumantha Rao Marepalli,[†] Octavian Antohi,[†] Jeffrey M. Becker,[‡] and Fred Naider*,[†]

Contribution from the Department of Chemistry, The College of Staten Island, and The Graduate School of The City University of New York, Staten Island, New York 10314, and Department of Microbiology and Department of Biochemistry, Cellular and Molecular Biology, University of Tennessee, Knoxville, Tennessee 37996

Received December 15, 1995[⊗]

Abstract: The structural features of model N^{α}-acetyl carboxyl-amide cyclic tetrapeptides with the sequence Xxx-Pro-Gly-Zzz where Xxx = Lys, Orn, Dab, and Dpr; Zzz = Glu and Asp (Dab, α, γ-diaminobutyric acid; Dpr, α,β-diaminopropionic acid) were studied to examine the influence of side chain lactamization on the stereochemical freedom of the backbone residues in *i* to *i* + *3* systems. Some of these cyclic peptides separate into distinct isomers at room temperature as evidenced by HPLC and NMR. Detailed analyses were carried out using 2D NMR and molecular modeling to unravel the structures of major conformers assumed by the cyclic peptides. Interproton distances obtained from ROESY spectra, amide proton temperature coefficients, backbone dihedral angles deduced from homonuclear coupling constants, and modeling studies (constrained annealing search, minimization, and dynamics simulations using the AMBER force field) suggest that in DMSO-d_6 solution these cyclic peptides adopt a variety of conformations that can be related to type II β-turns and γ-turns, but never to type I β-turns. The peptide backbone conformation, in this closely related series of cyclic peptides, is a function of the composition of the side chain but not the ring size.

1. Introduction

Cyclization of linear bioactive peptides is often attempted to reduce conformational freedom and, where possible, to preintroduce the receptor-induced preferred conformation of the molecule. The putative conformational homogeneity which results as a consequence of cyclization might lead to increased receptor specificity, increased agonist or antagonist potency, or extended resistance to enzymatic or proteolytic degradation.[1] Constraints attempted so far include chain end to chain end, side chain to chain end, and side chain to side chain cyclization. Cyclization involving backbone atoms has only been attempted infrequently.[2] Chain end to chain end cyclization often results in biologically inactive analogs due to the elimination of C- and N-termini interaction with the corresponding receptor

* To whom correspondence should be addressed.
[†] The City University of New York.
[‡] University of Tennessee.
[⊗] Abstract published in *Advance ACS Abstracts,* July 1, 1996.

(1) (a) Kessler, H. *Angew. Chem., Int. Ed. Engl.* **1982**, *21*, 512−523. (b) Hruby, V. J. *Life Sci.* **1982**, *31*, 189−199. (c) De Grado, W. F. *Adv. Protein Chem.* **1988**, *39*, 51−123. (d) Bitar, K. G.; Somogyvari-Vigh, A.; Coy, D. H. *Peptides* **1994**, *15*, 461−466. (e) Farlie, D. P.; Abbenate, G.; March, D. R. *Curr. Med. Chem.* **1995**, *2*, 654−686. (f) Sawyer, T. K. *Adv. Peptide-Based Drug Design;* Taylor, M. D., Amidon, G. L., Eds.; ACS Prof. Ref. Books, American Chemical Society: Washington, DC, 1995; pp 387−422. (g) Gulays, J.; Rivier, C.; Perrin, M.; Koerber, S. C.; Sutton, S.; Corrigan, A.; Lahrichi, S. L.; Craig, A. G.; Vale, W.; Rivier, J. *Proc. Natl. Acad. Sci. U.S.A.* **1995**, *92*, 10575−10579. (h) Arttamangkul, S.; Murray, T. F.; Delander, G. E.; Aldrich, J. V. *J. Med. Chem.* **1995**, *38*, 2410−2417.

(2) (a) Gilon, C.; Halle, D.; Chorev, M.; Selinger, Z.; Byk, G. *Biopolymers* **1991**, *31*, 745−750. (b) Hermkens, P. H. H.; Dinther, T. G. V.; Joukema, C. W.; Wagenaars, G. N.; Ottenheijm, H. C. J. *Tetrahedron Lett.* **1994**, *35*, 9271−9274.

S0002-7863(95)04217-X CCC: $12.00

(stereoelectronic effects).[3] On the other hand, both side chain to chain end and side chain to side chain cyclization have been quite successful. For example, side chain cyclization via cystine in the synthesis of an α-melanotropin analog[4] gave a super potent agonist and is now performed in many laboratories. Side chain to side chain *i* to *i* + *2* cyclization via amide bond formation was utilized to develop highly potent and selective opioid peptide analogs.[5−7] Similarly, *i* to *i* + *4* side chain lactamization has been employed to stabilize helical segments and yielded highly potent and metabolically stable growth hormone releasing factor analogs,[8,9] a human calcitonin analog,[10] and a potent parathyroid hormone-related protein antagonist.[11] Furthermore, *i* to *i* + *3* lactam bridging gave high affinity and selectivity for cholecystokinin analogs,[12−14] increased anticoagulant activity in a thrombin binding hirudin analog,[15] and enhanced antagonist potency in luteinizing hormone-releasing hormone.[16,17] Despite these successes the exact relationship between the size of the lactam ring and the conformation of the constrained region has not been systematically examined for *i* to *i* + *3* side chain lactamization of turn regions in peptides.

Mating in *Saccharomyces cerevisiae* offers an excellent paradigm to investigate peptide hormone−receptor interactions.[18] This yeast produces two peptide mating pheromones, one of which is α-factor, a tridecapeptide (WHWLQLKPGQPMY). To initiate signal transduction, α-factor binds to a receptor that is a member of the seven transmembrane G-protein coupled receptor family. As part of our efforts to elucidate the biologically active conformation of this peptide, we have synthesized stereochemically restricted analogs in which the side chains of residues 7 and 10 are linked by an amide bond. Our studies revealed that the biological activity and receptor binding affinity of these analogs are related to the size and composition of the lactam ring in the center of the pheromone.[19] In order to relate these biological results to the conformation of the lactam and to study the conformational freedom in peptides containing side chain to side chain amide bonds, we have synthesized N^{α}-acetyl carboxyl-amide terminal cyclic tetrapeptides with an XxxProGlyZzz sequence where Xxx = Lys, Orn, Dab, and Dpr and Zzz = Glu and Asp.[20] Initial characterization efforts revealed the presence of multiple conformers in these constrained model compounds. CD studies in water, trifluoroethanol and methanol suggest that the cyclic peptides exist in β-turn like conformations, likely involving the central Pro-Gly dipeptide.[20] Cyclo[1,4][Ac-Dab-Pro-Gly-Glu-NH_2] appears to assume a type II β-turn based on comparison with CD spectra calculated for idealized β-turns. The other peptides in the series probably exist as distorted versions of this conformation. The analysis of the CD curves was complicated by the fact that CD spectra are additive in nature and these peptides exist as mixtures of different conformers. To provide definitive information on the structures assumed by individual conformers these model compounds were subjected to biophysical analyses using 2D NMR and molecular modeling. In the present communication we present a detailed picture of different solution structures of the major conformers of these *i* to *i* + *3* cyclized model peptides.

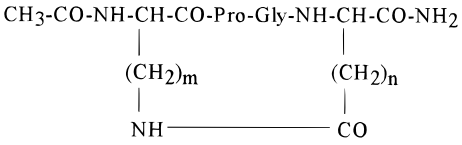

Peptide			Amino acid in Position	
			i	*i+3*
$Tetra_{42}$	m = 4;	n = 2	Lys	Glu
$Tetra_{32}$	m = 3;	n = 2	Orn	Glu
$Tetra_{22}$	m = 2;	n = 2	Dab	Glu
$Tetra_{12}$	m = 1;	n = 2	Dpr	Glu
$Tetra_{41}$	m = 4;	n = 1	Lys	Asp
$Tetra_{31}$	m = 3;	n = 1	Orn	Asp
$Tetra_{21}$	m = 2;	n = 1	Dab	Asp
$Tetra_{11}$	m = 1;	n = 1	Dpr	Asp

Figure 1. Primary structure of cyclic peptides ($Tetra_{42}$ to $Tetra_{11}$).

2. Materials and Experimental Methods

1. Synthesis. Peptides examined in this study were all more than 99% homogeneous and were characterized by HPLC, FABMS, and NMR spectroscopy.[20] These peptides are all cyclic tetrapeptides and have L-amino acids. They are named as $Tetra_{xx}$ where the suffix *xx* indicates the number of CH_2 groups on the side chains of first and fourth residues, respectively. For example cyclo[1,4][Ac-Lys-Pro-Gly-Glu-NH_2] is designated $Tetra_{42}$ whereas cyclo[1,4][Ac-Dpr-Pro-Gly-Asp-NH_2] is designated $Tetra_{11}$ (Figure 1).

2. NMR procedures. NMR spectra were acquired in DMSO-d_6 on a Varian Unityplus 600-MHz NMR spectrometer. Peptides dried in an Abderhalden drying pistol over refluxing methanol under high vacuum for 72 h were used for the NMR studies. DMSO-d_6 (100%) from Aldrich (Milwaukee, WI) was used to make solutions for NMR studies. TMS was used as the internal reference for proton resonances. Carbon chemical shifts were referenced against DMSO-d_6 at 39.5 ppm. Solutions of 0.5−20 mM peptides were used for assessing aggregation and 5 mM solutions for all conformational analyses. One-dimensional ^{1}H-NMR spectra for determining temperature coefficients were obtained at 295−325 K in increments of 5 K. Sample temperatures were controlled with the variable-temperature unit of the instrument.

(3) Bankowski, K.; Manning, M.; Seto, J.; Haldar, J.; Sawyer, W. H. *Int. J. Peptide Protein Res.* **1980**, *16*, 382−391.
(4) Sawyer, T. K.; Hruby, V. J.; Darman, P. A.; Hadley, M. E. *Proc. Natl. Acad. Sci. U.S.A.* **1982**, *79*, 1751−1755.
(5) Schiller, P. W.; Nguyen, T. M. D.; Lemieux, C.; Maziak, L. A. *J. Med. Chem.* **1985**, *28*, 1766−1771.
(6) Schiller, P. W.; Nguyen, T. M. D.; Maziak, L. A.; Wilkes, B. C.; Lemieux, C. *J. Med. Chem.* **1987**, *30*, 2094−2099.
(7) Mierke, D. F.; Schiller, P. W.; Goodman, M. *Biopolymers* **1990**, *29*, 943−952.
(8) Felix, A. M.; Heimer, E. P.; Wang, C. T.; Lambros, T. J.; Fournier, A.; Mowels, T. F.; Maines, S.; Campbell, R. M.; Wegrzynski, B. B.; Toome, V.; Fry, D.; Madison, V. S. *Int. J. Peptide Protein Res.* **1988**, *32*, 441−454.
(9) Fry, D. C.; Madison, V. S.; Greeley, D. N.; Felix, A. M.; Heimer, E. P.; Frohman, L.; Campbell, R. M.; Mowels, T. F.; Toome, V.; Wegrzynski, B. B. *Biopolymers* **1992**, *32*, 649−666.
(10) Kapurniotu, A.; Taylor, J. W. *J. Med. Chem.* **1995**, *38*, 836−847.
(11) Chorev, M.; Roubini, E.; McKee, R. L.; Gibbons, S. W.; Goldman, M. E.; Caulfield, M. P.; Rosenblatt, M. *Biochemistry* **1991**, *30*, 5968−5974.
(12) Charpenteir, B.; Pelaprat, D.; Durieux, C.; Dor, A.; Reibaud, M.; Blanchard, J. C.; Roques, B. P. *Proc. Natl. Acad. Sci. U.S.A.* **1988**, *85*, 1968−1972.
(13) Charpenteir, B.; Durieux, C.; Pelaprat, D.; Dor, A.; Reibaud, M.; Blanchard, J. C.; Roques, B. P. *Peptides* **1988**, *9*, 835−841.
(14) Charpenteir, B.; Dor, A.; Roy, P.; England, P.; Pham, H.; Durieux, C.; Roques, B. P. *J. Med. Chem.* **1989**, *32*, 1184−1190.
(15) Ning, Q.; Ripoll, D. R.; Szewczuk, Z.; Konishi, Y.; Ni, F. *Biopolymers* **1994**, *34*, 1125−1137.
(16) Bienstock, R. J.; Koerber, S. C.; Rizo, J.; Rivier, J. E.; Hagler, A. T.; Gierasch, L. M. *Peptides: Chemistry and Biology, Proceedings of Twelfth American Peptide Symposium;* Smith, J. A., Rivier, J. E., Eds.; ESCOM: Leiden, 1992; pp 262−264.
(17) Reddy, D. V.; Jagannadh, B.; Dutta, A. S.; Kunwar, A. C. *Int. J. Peptide Protein Res.* **1995**, *46*, 9−17.
(18) Sprague, G. F.; Thorner, J. W. *Molecular and Cellular Biology of the Yeast Saccharomyces, in Gene Expression*; Jones, E. W., Pringle, J. R., Broach, J. R., Eds.; Cold Spring Harbor Laboratory Press: Cold Spring Harbor, NY, 1992; Vol. 2, pp 657−744.
(19) Yang, W.; McKinney, A.; Becker, J. M.; Naider, F. *Biochemistry* **1995**, *34*, 1308−1315.
(20) Marepalli, H. R.; Yang, W.; Joshua, H.; Becker, J. M.; Naider, F. *Int. J. Peptide Protein Res.* **1995**, *45*, 418−429.

Complete proton resonance assignments were made[20] using COSY, RELAYED-COSY, and TOCSY experiments. HMQC and HMQC-TOCSY were used to assign unambiguously proton resonances of the conformationally heterogeneous cyclic tetrapeptides. ROESY[21] experiments were used to extract interproton distances. ROESY spectra were acquired at 300 K in phase-sensitive mode using the method of States *et al.*[22] Spectra were collected with 2K data blocks for 512 t_1-increments with a relaxation delay of 1.5 s and 64 transients for each t_1-increment. The spectral width in both dimensions was 6000 Hz. ROESY spectra were obtained using 32° flip angle spin lock pulses and resonance offset compensation to suppress HOHAHA contributions.[23] The effective field strength for spin lock is 1.9 kHz. The ROESY spectra were recorded with five different mixing times, *viz.* 50, 100, 150, 200, and 250 ms, to generate ROE buildup curves. The ROE intensities obtained at 100 ms mixing time were found to be in the middle of the linear curves. Therefore, interproton distances were deduced from ROESY experiments carried out with 100 ms mixing time.

NMR data, acquired on a Varian spectrometer, were processed on a SUN sparc station *IPX* using vnmr software. Prior to Fourier transformation, ROESY time domain data were apodized using shifted sine-bell or Gaussian window functions in both dimensions and zero filled to 2K × 2K real points. Multiplication of the first t_1-increment by 0.5 prior to the second Fourier transformation was carried out to reduce the t_1 ridges in all ROESY spectra.

3. Modeling Procedures. (a) Vacuum Structures. The N^{α}-acetyl, carboxyl-amide, 1−4 side chain cyclized tetrapeptides structures were built with the BIOPOLYMER module of the SYBYL software on an INDIGO2 SGI and then minimized using the AMBER force field. The amino acid models Lys, Orn, Dab, Dpr, Asp and Glu, used in cyclizations were custom made to be recognized by the AMBER force field using the dictionary options of the SYBYL package. Constrained searches and minimizations were conducted using the annealing procedure in SYBYL (consecutive dynamics at $T = 500$ and 20 K) starting with the minimized structures. The constraints were input as ranges centered on the experimentally determined distance (±10% of the distance value). The results were analyzed and the conformations compatible with the experimental data were identified and further searched and minimized.

(b) Solvent Box and Solvated Tetrapeptides. The DMSO molecule was optimized by *ab initio* calculations using the 6-31G* basis set. The resulting parameters (*i.e.*, charges: C, −0.703; S, 0.944; O, −0.784; H, 0.221, 0.213, 0.188; bond lengths and bond angles: SC, 1.80 Å; SO, 1.49 Å; CH, 1.10 Å; CSC, 97.7°; CSO, 106.7°; SCH, 109.5°) were introduced into the Kollman All-Atom parameter set of the SYBYL software. A DMSO box of molecules having these parameters was built and minimized using the AMBER (Kollman All-Atom) force field. This box was subsequently used to generate the solvent environment for the cyclic tetrapeptide computations. We used parallelepipedic (almost cubic) boxes. The typical length of a solvent box side was between 32 and 36 Å and contained around 325 molecules of solvent. The best (lowest energy) vacuum minimized structures resulting from the searches were solvated and minimized with periodic boundary conditions.

(c) Dynamics. Constrained Molecular Dynamics (MD) simulations in vacuum and DMSO were performed on the eight tetrapeptides using the AMBER force field and the Verlet algorithm. The simulations were carried out at constant temperature under canonical ensemble conditions and were started from well-minimized structures obtained as explained above. The final temperature of 300 K was reached in three steps: heating at 1000 K for 1 ps, cooling at 500 K for 5 ps, equilibration at 300 K for 14 ps, and simulations at 300 K for 60 ps.[24] The equations of motion integration step was 1 and snapshots were taken every 60 fs. For $Tetra_{42}$, which is the largest molecule among our model peptides, simulations were carried out with the same algorithm with an averaging period of 120 ps. There were no significant differences from the 60-ps results. Averages for the quantities of interest (distances and dihedral angles) were computed over the simulation (60 ps) periods and compared to the experimental data and are presented in the text (Table 4) and in the supporting information (Tables S1−S8).

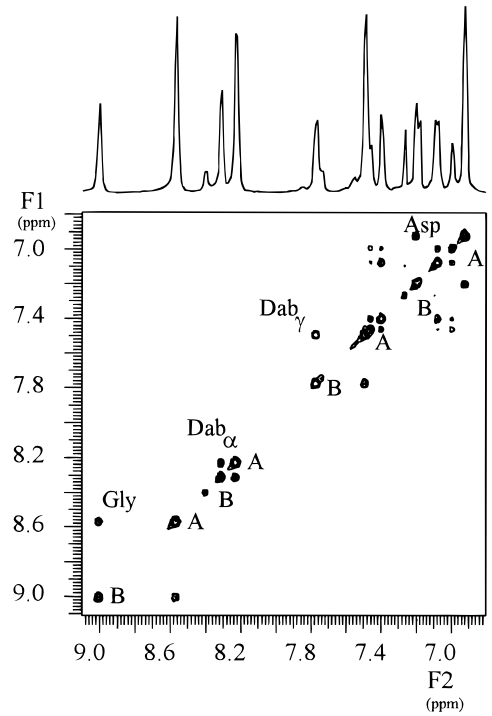

Figure 2. Amide region of the 600-MHz ROESY spectrum of $Tetra_{21}$ showing *NH*/*NH* exchange cross peaks (same sign as the diagonal) of interconverting conformers, isomer **A** and isomer **B**. Exchange cross peaks for isomer **C** were not observed at this contour level due to its low relative concentration. The 1D spectrum is presented at the top of the ROESY spectrum.

3. Results

1. Aggregation Studies of Cyclic Peptides. The primary structures of cyclic peptides $Tetra_{42}$ to $Tetra_{11}$ are shown in Figure 1. One-dimensional proton NMR spectra for each of the cyclic tetrapeptides over a concentration range of 0.5 to 20 mM peptide were recorded. The observed proton chemical shifts as well as spectral line widths in this concentration range were essentially invariant allowing us to conclude that intermolecular association was absent over the concentration range tested (data not shown).

2. Conformational Heterogeneity in *i* to *i* + *3* Monomeric Lactams. Initial NMR analyses of these cyclic peptides showed one predominant resonance for each amide *NH* in $Tetra_{42}$, $Tetra_{41}$, $Tetra_{32}$, and $Tetra_{31}$ suggesting either one dominant isomer or fast conformational averaging on the NMR time scale.[20] In contrast, the coexistence of slowly interconverting multiple conformers in $Tetra_{22}$, $Tetra_{21}$, $Tetra_{12}$, and $Tetra_{11}$ peptides was established by *NH*/*NH* and $C^{\alpha}H/C^{\alpha}H$ exchange cross-peaks (same sign as the diagonal) in their corresponding ROESY spectra. The *NH*/*NH* exchange cross peaks of major isomers **A** and **B** for $Tetra_{21}$ are shown in Figure 2. Overlaid on this spectrum is the corresponding 1D spectrum. Heating the samples resulted in collapse of the multiple peaks to single resonances for each *NH* and $^{\alpha}CH$ proton. This effect was reversible upon cooling the samples and unequivocally establishes the occurrence of slowly interconverting conformers in these peptides (data not shown).

(21) (a) Bothner-By, A. A.; Stephens, R. L.; Lee, J.; Warren, C. D.; Jeanloz, R. W. *J. Am. Chem. Soc.* **1984**, *106*, 811−813. (b) Bax, A.; Davis, D. G. *J. Magn. Reson.* **1985**, *63*, 207−213.

(22) States, D. J.; Haberkorn, R. A.; Ruben, D. J. *J. Magn. Reson.* **1982**, *48*, 286−292.

(23) (a) Kessler, H.; Griesinger, C.; Kerssebaum, R.; Wagner, K.; Ernst, R. R. *J. Am. Chem. Soc.*, **1987**, *109*, 607−609. (b) Griesinger, C.; Ernst, R. R. *J. Magn. Reson.* **1987**, *75*, 261−271.

(24) Matter, H.; Kessler, H. *J. Am. Chem. Soc.* **1995**, *117*, 3347−3359.

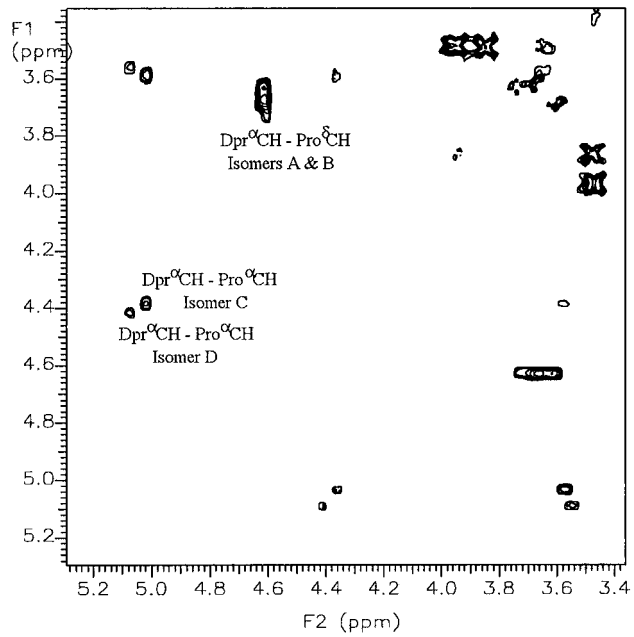

Figure 3. Part of the 600-MHz ROESY spectrum of Tetra$_{12}$ showing (i) the Dpr$^{\alpha}$CH−Pro$^{\delta}$CH cross peak for isomer **A** and isomer **B** indicating a *trans* Dpr−Pro peptide bond and (ii) the Dpr$^{\alpha}$CH−Pro$^{\alpha}$-CH cross peaks for isomer **C** and isomer **D** indicating a *cis* Dpr−Pro peptide bond.

Table 1. Temperature Coefficients of *NH* Protons ($-\Delta\delta/\Delta T$, ppb/K) of Cyclic Peptides Tetra$_{42}$ to Tetra$_{11}$ in DMSO-d_6

tetrapeptide	$^{\alpha}$NH(i)	$^{\omega}$NH(i)	$^{\alpha}$NH($i+2$)	$^{\alpha}$NH($i+3$)
Tetra$_{42}$	7.02	5.89	3.14	4.80
Tetra$_{32}$	7.44	2.28	6.76	0.90
Tetra$_{22}$[a]	7.44	5.71	7.57	−1.80
Tetra$_{12}$[a]	4.40	3.99	0.82	0.22
Tetra$_{41}$	5.91	3.33	5.63	0.72
Tetra$_{31}$	5.30	5.40	3.45	2.65
Tetra$_{21}$[a]	4.54	3.72	4.04	−1.40
Tetra$_{11}$[a]	4.15	3.10	3.40	−0.90

[a] Major conformer.

Tetra$_{11}$ exhibited two isomers (**A** and **B**) in a 6:1 ratio. While Tetra$_{22}$ and Tetra$_{21}$ showed the presence of three isomers (**A**, **B**, and **C**) in 16:3:1 and 32:23:1 ratios, respectively.[20] The NMR spectrum of Tetra$_{12}$ revealed the existence of four isomers (**A**, **B**, **C**, and **D**) in a 20:6:4:1 ratio.[20] Isomer **A** of Tetra$_{11}$ and Tetra$_{21}$ and both isomers **A** and **B** of Tetra$_{12}$ and Tetra$_{22}$ adopt a *trans* configuration with respect to the Xxx−Pro peptide bond as indicated by characteristic ROE cross peaks from the XxxC$^{\alpha}$H to the ProC$^{\delta}$H protons. A *cis* configuration in isomer B of Tetra$_{21}$ and both isomers **C** and **D** of Tetra$_{12}$ was evidenced by XxxC$^{\alpha}$H and ProC$^{\alpha}$H cross peaks in their ROESY spectra. This is illustrated for Tetra$_{12}$ in Figure 3. Nothing can be definitely said regarding isomers **C** in both the Tetra$_{21}$ and Tetra$_{22}$ due to a lack of cross peaks. All of the conformationally homogeneouspeptides (Tetra$_{42}$, Tetra$_{41}$, Tetra$_{32}$, and Tetra$_{31}$) exhibited a *trans* Xxx−Pro peptide bond. In the present investigation solution structures were elucidated only for the *trans* isomers in each of the cyclic peptides. In the case of the conformationally heterogeneous peptides (Tetra$_{22}$, Tetra$_{21}$, Tetra$_{12}$, and Tetra$_{11}$) the major *trans* isomer was examined.

3. Temperature Gradients of amide *NH*s. The temperature coefficients for amide protons were calculated by a least-squares analysis of the temperature dependence of their resonances (Table 1). The *cis*/*trans* isomers for the tetrapeptides (Tetra$_{22}$, Tetra$_{21}$, Tetra$_{12}$, and Tetra$_{11}$) are conformationally distinct over the temperature range which is used for calculating temperature coefficients. Temperature coefficients for the major *trans* isomer of each peptide are presented in Table 1. The $^{\alpha}$NH of the *i* residue is outside the cyclic system and is expected to be solvent exposed. As anticipated its temperature coefficient is the highest value (4.15−7.44 ppb/K) in each peptide. The temperature coefficient of the $i+3$ residue $^{\alpha}$NH is very low in seven of the eight cyclic peptides indicating its probable involvement in intramolecular H bonding. The exception is the 18-membered cyclic peptide, Tetra$_{42}$, which has a coefficient of 4.8 ppb/K. Each of these protons except in Tetra$_{42}$ resonate up field (6.95−7.32 ppm) compared to other *NH*s in their corresponding peptides.[20] This suggests that these $^{\alpha}$*NH*s are not solvated by DMSO.[25] The temperature coefficient of the Asp $^{\alpha}$*NH* in the Asp-containing tetrapeptides was found to be highest for Tetra$_{31}$ followed by Tetra$_{41}$ and Tetra$_{11}$ while it is smallest for Tetra$_{21}$ (Table 1). We noticed a corresponding upfield shift of the Asp $^{\alpha}$*NH* in these peptides (7.32, 7.26, 7.03, and 6.83 ppm, respectively).[20] A similar trend was observed in the Glu-containing tetrapeptides. With the exception of Tetra$_{42}$ these observations further support the involvement of the $i+3$ $^{\alpha}$*NH* in an intramolecular hydrogen bond. We also observed that the temperature coefficient of the $i+2$ residue $^{\alpha}$NH is exceptionally low in Tetra$_{12}$ (0.82 ppb/K) implying either that it is strongly shielded from solvent or that it participates in a relatively stable H-bond. In Tetra$_{42}$, Tetra$_{31}$, and Tetra$_{11}$ the moderately low coefficient of the $i+2$ $^{\alpha}$*NH* (∼3 ppb/K) also suggests moderate solvent shielding or participation in H bonding. Similarly, the lactam *NH* displayed a relatively low ($-\Delta\delta/\Delta T$) coefficient in only one cyclic peptide (Tetra$_{32}$, 2.28 ppb/K) and moderately low values in another four peptides, suggesting that these amide protons were moderately solvent shielded.

4. $^3J_{NH-C^{\alpha}H}$ Coupling Constants and Backbone Dihedral Angles Derived from Coupling Constants and Modeling. The $^3J_{NH-C^{\alpha}H}$ coupling constants were extracted from well-digitized 1D proton spectra. The resolution of the spectra was enhanced by applying a Gaussian window function prior to Fourier transformation. Bystrov's Karplus equations[26] were used to calculate the dihedral angles (ϕ) from these coupling constants (see the supporting information, Table S8). The average dihedral angles computed from the 60-ps simulations in DMSO are generally within ±30° of at least one of the values derived from the coupling constants.

5. Ramachandran Plots. The dihedral angles of the turn region (ϕ_2, ψ_2, ϕ_3, and ψ_3) obtained by averaging over the 60-ps dynamics simulations are tabulated along with the temperature coefficients of $^{\alpha}$*NH*($i+3$) and two incisive interproton distances in Table 2. The ϕ_2 dihedral angle is constrained to be around −60° by the pyrrolidine ring of the proline residue at position $i+1$. For Tetra$_{42}$ and Tetra$_{31}$ the ψ_2 dihedral angle is more than 20° lower than the value corresponding to a type II β-turn (120°). The average value of the backbone dihedral angles for Pro of Tetra$_{42}$ corresponds to an inverse γ-turn around this residue ($i+1$ position, Table 2). The dihedral angles for 1000 discrete steps of the molecular dynamics simulation are shown in a Ramachandran map (Figure 4A) and cluster near the values expected for the inverse γ-turn. The Ramachandran plot of the Gly residue in Tetra$_{32}$ is consistent with the presence of a γ-turn around this residue (Figure 4B; Table 2). Interestingly, Tetra$_{31}$ has ϕ,ψ angles of Pro similar to those of Tetra$_{42}$

(25) (a) Pease, L. G.; Deber, C. M.; Blout, E. R. *J. Am. Chem. Soc.* **1973**, *95*, 258−260. (b) Rizo, J.; Koerber, S. C.; Bienstock, R. J.; Rivier, J.; Hagler, A. T.; Gierasch, L. M. *J. Am. Chem. Soc.* **1992**, *114*, 2852−2859.

(26) (a) Karplus, M. J. *J. Chem. Phys.* **1959,** *30*, 11−15. (b) Bystrov, V. F. *Prog. Nucl. Magn. Reson. Spectrosc.* **1976,** *10*, 41−81.

Table 2. Conformational Characteristics of Cyclic Tetrapeptides from NMR and Modeling[a]

peptides and ideal turns	Gly$^{\alpha}_{NH}$−Zzz$^{\alpha}_{NH}$		Pro$^{\alpha}_{CH}$−Gly$^{\alpha}_{NH}$		temp coef	H-bonding	dihedral angles (modeling),[e] deg			
	ROESY dist, Å	modeling dist, Å	ROESY dist, Å	modeling dist, Å	Zzz$^{\alpha}_{NH}$, ppb/K	H-bond dist modeling, Å	ϕ_2	ψ_2	ϕ_3	ψ_3
Tetra$_{42}$		4.74(0.18)	2.20	2.22(0.06)	4.80		−77(9)	82(10)	108(21)	178(9)
Tetra$_{32}$	3.40	3.49(0.10)	2.20	2.31(0.07)	0.90	2.06[c]	−68(11)	160(7)	81(8)	−68(8)
Tetra$_{22}$[b]	2.69	2.77(0.10)	2.19	2.18(0.08)	−1.80	2.47[d]	−71(7)	126(5)	87(9)	5(3)
Tetra$_{12}$[b]	2.70	2.69(0.08)	2.65	2.54(0.05)	0.22	2.46[c,d]	−65(22)	128(29)	68(10)	19(9)
Tetra$_{41}$	2.80	2.83(0.09)	2.29	2.26(0.05)	0.72	2.75[d]	−77(12)	142(18)	53(9)	19(10)
Tetra$_{31}$	3.30	3.42(0.07)	2.41	2.32(0.08)	2.65	1.95[c]	−46(10)	99(9)	80(9)	−52(9)
Tetra$_{21}$[b]	2.85	2.84(0.09)	2.34	2.24(0.06)	−1.40	2.50[c]	−95(10)	133(10)	67(9)	30(12)
Tetra$_{11}$[b]	2.84	2.88(0.11)	2.48	2.34(0.07)	−0.90	2.64[d]	−73(8)	112(10)	72(10)	21(10)
Type II β-turn	2.40		2.20		<2.5	2.5	−60	120	80	0
Type I β-turn	2.40		3.40		<2.5	2.5	−60	−30	−90	0
γ-turn	3.70		2.30		<2.5	2.5			70 to 85	−60 to −70
γ'-turn					<2.5	2.5	−60 to −70	70 to 85		

[a] Root-mean-square deviation is given in parentheses for each interproton distance and torsion angle obtained from modeling. [b] Major conformer. [c] 1 ← 3 H bonding. [d] 1 ← 4 H bonding. [e] Dihedral angles extracted from 60 ps MD trajectories in DMSO.

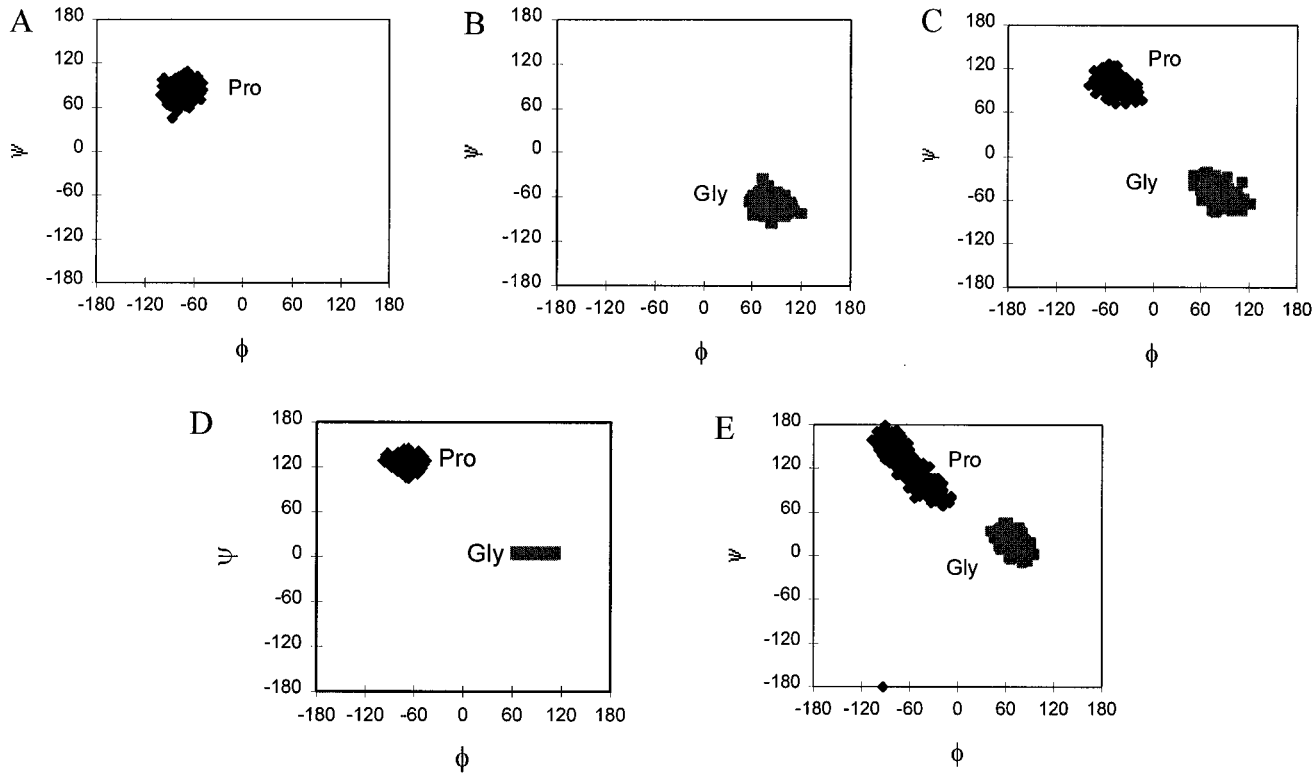

Figure 4. Ramachandran maps of the backbone dihedral angles of the DMSO dynamics structures: (A) Tetra$_{42}$; (B) Tetra$_{32}$; (C) Tetra$_{31}$; (D) Tetra$_{22}$; and (E) Tetra$_{12}$. Dihedral angles (ϕ,ψ) for the Pro and/or Gly residues from 1000 discrete conformers observed during a 60-ps simulation are included in the plot.

and ϕ,ψ angles of Gly similar to those of Tetra$_{32}$, implying the presence of both conformational features in this molecule (Figure 4C; Table 2). On the other hand, the Ramachandran maps of Pro(i + *1*) and Gly(i + *2*) dihedral angles in Tetra$_{22}$ agree with a very good type II β-turn (Figure 4D, Table 2). In Tetra$_{12}$ the ϕ,ψ of both the Pro and the Gly are spread over the type II β-turn and both the γ- and γ'-turn regions (Figure 4E) suggesting the coexistence of several important conformations in the major isomer of this tetrapeptide. Tetra$_{21}$ exhibits the largest distortion for the Pro ϕ (−95° average on the solvent simulation). This indicates significant strain for the prolyl residue and may correlate with the fact that this molecule exhibits the largest percentage of *cis* isomer for any tetrapeptide (41%).

6. Interproton Distances Deduced from ROE Intensities and from Modeling. Low spin-lock field strength and small (32°) flip angle pulses for the mixing sequence were used while acquiring the ROESY spectra to minimize HOHAHA contributions.[23] The position of the offset was also chosen in such a way so that the *J*-coupling contributions are minimal. ROESY spectra with mixing times of 50, 100, 150, 200, and 250 ms were used to obtain ROE buildup curves (Figure 5). Average ROE intensities from both sides of the diagonal were used. The dependence of the ROE integrals on mixing time was seen to be approximately linear up till 150 ms. Assuming isotropic mobility and the isolated two-spin approximation (ISPA),[27] the observed average integrals from 100-ms ROESY spectra were converted to interproton distances. The obtained distances were calibrated with respect to the distance between Gly methylenic protons (1.77 Å). Both intra- and interresidue ROESY cross peaks were obtained for all of the cyclic tetrapeptides. The *NH*−*NH*(i + *2*; i + *3*) interproton distance is the crucial distance which indicates the occurrence of a β-turn or a γ-turn. This is expected to be around 2.4 Å for both type I and type II β-turns

(27) Neuhaus, D.; Williamson, M. *The Nuclear Overhauser Effect in Structural and Conformational Analysis*; VCH: Weinheim, FRG, 1989.

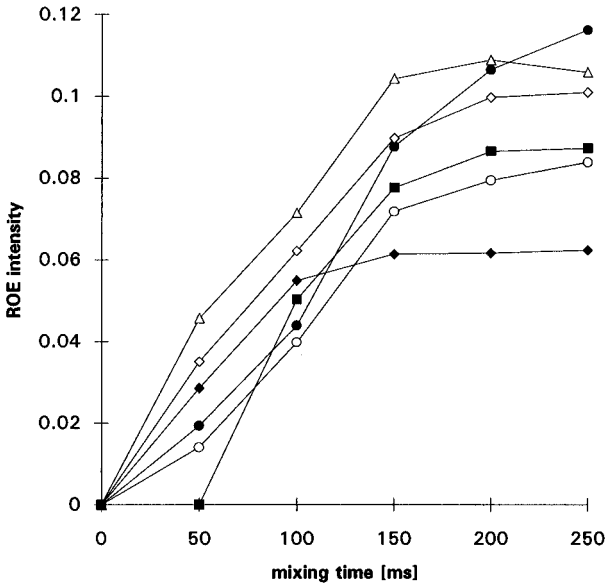

Figure 5. ROE buildup curves for a few important interproton distances of $Tetra_{12}$: (●) $d_{\alpha N}(i+1,i+2)$; (○) $d_{NN}(i+2,i+3)$; (◇) $d_{N\beta}\beta(i,i+3)$; (◆) $d_{N\beta}\gamma(i,i+3)$; (△) $d_{N\beta}\gamma(i,i+3)$; (■) $d_{N}\gamma(i+3,i+3)$.

Table 3. Comparison between the ROE Distance Values and the Simulated Average Distance Values

	root-mean-square deviation, (Å/dist)	
tetrapeptide	in vacuum	in DMSO
$Tetra_{42}$	0.050	0.047
$Tetra_{32}$	0.031	0.033
$Tetra_{22}$[a]	0.024	0.026
$Tetra_{12}$[a]	0.033	0.037
$Tetra_{41}$	0.052	0.043
$Tetra_{31}$	0.029	0.029
$Tetra_{21}$[a]	0.036	0.039
$Tetra_{11}$[a]	0.029	0.027

[a] Major conformer.

and around 3.70 Å for a γ-turn. $Tetra_{42}$ is unique in this series of cyclic peptides in that its spectrum was devoid of this ROE cross peak (Table 2). The $NH-NH(i+2; i+3)$ distance was found to be between 3.40 and 3.30 Å for $Tetra_{32}$ and $Tetra_{31}$, respectively, and between 2.70 and 2.85 Å for the remaining peptides. An important interproton distance that discriminates a type I β-turn from type II β- and γ-turns is $^{\alpha}CH-^{\alpha}NH(i+1; i+2)$. This is expected to be around 3.40 Å for a type I β-turn and between 2.20 and 2.30 Å for both a type II β-turn and a γ-turn. ROE measurements for all peptides yielded a shorter distance (around 2.20−2.65 Å) between these two atoms, indicating the presence of type II β-turns and/or γ-turns. These measurements allow us to rule out the existence of type I β-turn-like conformations in any of the cyclic peptides.

Among the vacuum structures generated for these cyclic peptides, only those which satisfied NMR derived interproton distances (root mean square deviation being less than 0.055 Å/distance, Table 3) and temperature coefficients are selected for further studies in solvent. These structures were solvated with DMSO, then further minimized, and dynamics simulations were carried out (*vide supra*). The modeling distances and dihedral angles are presented in Table 2 where the NMR distances and modeling distances are also compared. The values from the modeling represent average values extracted from a 60-ps molecular dynamics simulation in DMSO. In general, the average solvent dynamics values were in good agreement with the ROE distances (a root-mean-square deviation of less than 0.05 Å/distance, Table 3). The relevance of the distance and dihedral angles to the conformations of the *i* to $i+3$ lactams is given in the Discussion section.

4. Discussion

β-turns are a commonly reported conformational feature that have been associated with the biologically active state of many peptides.[28] In particular, a Pro-Gly sequence often occurs in type II β-turns[29] and cyclization is attempted in many laboratories to eliminate conformational heterogeneity of linear peptides. The peptides involved in the present study are both cyclic and possess a central Pro-Gly dipeptide unit. Hence all of these cyclic tetrapeptides are expected to manifest a type II β-turn as their conformational feature if the side chain length variation and/or ring size has no influence on backbone conformation. The NMR and modeling studies reported herein suggest that the stereochemical situation is considerably more complex for *i to* $i+3$ cyclization around a central Pro-Gly unit.

1. Peptide Conformations. Turns occur in peptides and proteins when a growing peptide chain folds back on its backbone. A 10-membered H-bonded ring comprising the carbonyl of the *i*th residue and the amide *NH* of the $i+3$ residue is defined as a β-turn.[30] An interprotonic distance of 2.40 Å between the $^{\alpha}$NHs of the $i+2$ and $i+3$ residues is expected for both type I and II β-turns. The proximity of the $C^{\alpha}H(i+1)$ to the $^{\alpha}NH(i+2)$, 3.40 and 2.20 Å, respectively, discriminates between type I and II β-turns. Type I and II β-turns also differ in their torsion angles ψ_2 and ϕ_3 which are −30°,−90° and 120°,80°, respectively. The differences reflect opposite orientations of the $i+1$ carbonyl group with respect to the plane of the 10-membered ring. On the other hand, a 7-membered H-bonded ring between the carbonyl of *i*th residue and amide *NH* of the $i+2$ residue results in a γ-turn around the $i+1$ residue. The interproton distance between $^{\alpha}$NHs of the $i+1$ and $i+2$ residues is 3.40 Å and the backbone dihedral angles ϕ and ψ of the $i+1$ residue about which the γ-turn is located are 70° to 85° and −60° to −70°, respectively.[31]

We have used the above considerations to model solution structures for a series of cyclic tetrapeptides using NMR-derived constraints. The Ramachandran plots of the critical dihedral angles give a clear representation of the variations found in an ensemble of 1000 structures. The rms deviations for the average distance and the torsional angle in these ensembles are presented in Tables 2−4 in the paper and Tables S1−S8 in the supporting information. The average interproton distances obtained from the analysis of the vacuum and DMSO simulations of these peptides are in very good agreement with their corresponding ROE derived distances (Tables 4 and S1−S7). H-bonding patterns observed in the dynamics simulations of these molecules support the temperature coefficients obtained from NMR for

(28) (a) Veber, D. F. *Peptides: Synthesis, Structure and Function*; Rich, D. H., Gross, E., Eds.; Pierce Chemical Co.: Rockford, IL, 1981; pp 685-694. (b) Freidinger, R. M. *Peptides: Synthesis, Structure and Function*; Rich, D. H., Gross, E., Eds.; Pierce Chemical Co.: Rockford, IL, 1981; pp 673-683. (c) Sawyer, T. K.; Cody, W. L.; Knittle, J. J.; Hruby, V. J.; Hadley, M. E.; Hirsch, M. D.; O'Donohue, T. L. *Peptides: Structure and Function*; Hruby, V. J., Rich, D. H., Eds.; Pierce Chemical Co.: Rockford, IL, 1983; pp 323−331. (d) Schiller, P. W. *The Peptides*; Udenfriend, S., Meienhofer, J., Eds.; Academic Press: New York, 1984; Vol. 6, pp 219−268. (e) Hruby, V. J.; Al-Obeidi, F.; Kazmierski, W. M. *Biochem. J.* **1990**, *268*, 249−262. (f) Rizo, J.; Gierasch, L. M. *Annu. Rev. Biochem.* **1992**, *61*, 387−418.

(29) (a) Chou, P. Y.; Fasman, G. D. *Adv Enzymol.* **1978**, *47*, 45−148. (b) Gierach, L. M.; Deber, C. M.; Madison, V.; Niu, C-H.; Blout, E. R. *Biochemistry* **1981**, *20*, 4730−4738.

(30) (a) Venkatachalam, C. M. *Biopolymers* **1968**, *6*, 1425−1436. (b) Wüthrich, K. *NMR of Proteins and Nucleic Acids*; John Wiley & Sons, Inc.: New York, 1986; pp 117−129.

(31) (a) Nemethy, G.; Printz, M. P. *Macromolecules* **1972**, *5*, 755−758. (b) Smith, J. A.; Pease, L. G. *Crit. Rev. Biochem.* **1980**, 315−399.

Table 4. Comparison between the Experimental and Calculated Interproton Distances for $Tetra_{22}$[a–c]

protons	ROESY distance, Å[d]	MD av, Å in vacuum[e]	MD av, Å in DMSO[f]
Pro$^{\alpha}$CH-GlyNH	2.19	2.19(0.08)	2.18(0.08)
GlyNH-Gly$^{\alpha}$CH^{proR}	2.44	2.22(0.08)	2.20(0.08)
GlyNH-Gly$^{\alpha}$CH^{proS}	3.31	2.96(0.07)	2.99(0.06)
GluNH-Gly$^{\alpha}$CH^{proR}	3.06	3.24(0.06)	3.25(0.06)
GluNH-Gly$^{\alpha}$CH^{proS}	4.26	3.95(0.04)	3.90(0.05)
GlyNH-GluNH	2.69	2.76(0.10)	2.77(0.10)
GluNH-Glu$^{\alpha}$CH	2.97	2.99(0.05)	3.00(0.06)
GluNH-Glu$^{\gamma}$CH2	3.49	3.34(0.07)	3.35(0.08)
Glu$^{\alpha}$CH-Glu$^{\gamma}$CH1	2.38	2.53(0.07)	2.53(0.07)
Glu$^{\alpha}$CH-Glu$^{\gamma}$CH2	2.78	2.68(0.08)	2.72(0.10)
Dab$^{\gamma}$NH-Glu$^{\gamma}$CH2	2.29	2.22(0.08)	2.24(0.08)
Dab$^{\gamma}$NH-Dab$^{\gamma}$CH1	2.38	2.39(0.06)	2.40(0.06)
Dab$^{\gamma}$NH-Dab$^{\gamma}$CH2	3.13	2.99(0.04)	3.00(0.04)
Dab$^{\alpha}$CH-Dab$^{\gamma}$CH1	2.54	2.47(0.08)	2.46(0.08)
Dab$^{\alpha}$CH-Dab$^{\beta}$CH1	2.28	2.29(0.07)	2.31(0.08)
Dab$^{\alpha}$CH-Dab$^{\beta}$CH2	2.62	2.88(0.04)	2.88(0.04)
Dab$^{\alpha}$CH-Dab$^{\alpha}$NH	3.26	3.03(0.04)	3.57(0.12)
Dab$^{\alpha}$CH-Pro$^{\delta}$CH1	2.18	2.19(0.13)	2.25(0.14)
Dab$^{\alpha}$CH-Pro$^{\delta}$CH2	2.23	2.40(0.12)	2.38(0.13)

[a] Major conformer. [b] Diastereotopic assignments are given as superscripts. [c] Root-mean-square deviation is given in parentheses for each interproton distance obtained from modeling for $Tetra_{22}$. [d] Experimental data are extracted from a ROESY spectrum (100 ms) for $Tetra_{22}$ in DMSO at 300 K. [e] Calculated interproton distances are computed from 60-ps MD trajectories in vacuum for $Tetra_{22}$. [f] Calculated interproton distances are computed from 60-ps MD trajectories in DMSO for $Tetra_{22}$.

the corresponding amide *NH* protons (*vide infra*). However, careful scrutiny of the dynamics simulations shows that several of these cyclic peptides exist as ensembles of coexisting structures involving both β- and γ-turns. The conformation of each peptide is discussed separately below.

2. Cyclo^{1,4}[Ac-Lys-Pro-Gly-Glu-NH$_2$] ($Tetra_{42}$). This structure is unique in the series in that no ROESY cross peak is observed between the $i + 2$ (Gly) and $i + 3$ (Glu) *NH*'s (Table 2). The large (4.80 ppb/K) temperature coefficient of the $i + 3$ *NH* suggests that it points outside the cyclization ring and consequently the $i + 2$ residue of this tetrapeptide is far from adopting a type II β-turn conformation. On the other hand, the moderately low temperature coefficient of the Gly ($i + 2$) *NH* (3.14 ppb/K) suggests that this atom is somewhat solvent shielded or inside the lactam cycle. The MD simulation in both vacuum and DMSO revealed a 7-membered ring centered around Pro and closed by a hydrogen bond between the Gly *NH* and Lys CO (Figure 6A). The average ϕ and ψ angles of Pro, $-77°$ and 77°, respectively, in the vacuum simulation and $-77°$ and 82° in DMSO, correspond to a γ'-turn conformation. As seen in the simulation, except for this part of the molecule, the structure seems to be very flexible and few constraints were found in the ROESY analysis.

3. Cyclo^{1,4}[Ac-Orn-Pro-Gly-Glu-NH$_2$] ($Tetra_{32}$). The distinctive features of $Tetra_{32}$ are the large ROE distance (3.40 Å) between the *NH*'s at the $i + 2$ and $i + 3$ positions, the low temperature coefficient of the Glu *NH* (0.90 ppb/K), and the relatively low temperature coefficient of the lactam *NH* (2.30 ppb/K, the lowest of all side chain *NH*'s in the series). The vacuum and DMSO simulations based on the ROE constraints seem to accommodate these facts very well. The simulation revealed a very stable H-bond between the Glu *NH* and the CO of Pro that closes a 7-membered ring around Gly in a γ-turn-like conformation (Figure 6B). The average dihedral angles ϕ and ψ of Gly, 84° and $-68°$ in the vacuum simulation and 81° and $-68°$ in the DMSO simulation, correspond to a C_7 γ-turn conformation. The Glu *NH* also exhibited some ability to H bond to the side chain CO of Glu forming a transient intraresidue 7-membered ring. The side chain *NH* of ornithine formed an H bond with the acetyl CO. Although such interaction gives rise to a 9-membered ring that is outside the cyclization ring, this H bond was stable throughout the dynamics, and it provides the only possible rationale for the low temperature coefficient of this side chain amide bond.

4. Cyclo^{1,4}[Ac-Dab-Pro-Gly-Glu-NH$_2$] ($Tetra_{22}$). The Glu *NH* of this molecule exhibited the lowest temperature coefficient (-1.80 ppb/K) of the series while the remaining *NH*'s had high temperature coefficients (between 5.7 and 7.6 ppb/K; Table 1). The Pro $^{\alpha}$CH to Gly *NH* and Gly *NH* to Glu *NH* distances (2.19 and 2.70 Å, respectively) together with this very low *NH* temperature coefficient suggest that the backbone of this molecule adopts a relatively stable type II β-turn conformation. This conclusion agrees well with our CD results which were run in different solvents and reflect the average for all conformers of this peptide.[20] The average interproton distances obtained from the analysis of the vacuum and DMSO dynamics simulations of this molecule are in very good agreement with its ROE derived distances (Table 4). The dynamics showed a very stable H bond between the Glu *NH* and the Dab carbonyl. The average backbone dihedral angles ϕ and ψ of Pro and Gly are $-56°$, 122°, 82°, and 19°, respectively, in vacuum and $-71°$, 126°, 87° and 5°, respectively, in DMSO. They correspond to an almost perfect type II β-turn around the Pro and Gly residues (Figure 6D).

5. Cyclo^{1,4}[Ac-Dpr-Pro-Gly-Glu-NH$_2$] ($Tetra_{12}$). The distance between the Gly *NH* and the Pro $^{\alpha}$CH in the major isomer of this molecule is larger than in any other tetrapeptide (2.65 Å). The Gly *NH* also has the lowest temperature coefficient (0.82 ppb/K) of all Gly *NH*'s in the series (Table 1). Together these two facts suggest that in this conformer the Gly *NH* is oriented toward the lactam ring. The vacuum and solvent simulations show that this *NH* is able to H bond to the CO of Dpr forming a 7-membered ring that is highly populated during the evolutions. The temperature coefficient of the Glu *NH* is found to be 0.22 ppb/K also indicating strong H bonding. Indeed, both simulations show this *NH* forms hydrogen bonds with the carbonyls of Dpr (corresponding to a typical type II β-turn 10-membered ring) and Pro (a 7-membered ring around Gly) that are very stable throughout the dynamics. On the average, the molecule seems to adopt a type II β-turn and at the same time oscillates between two extreme conformations, one corresponding to a γ'-turn around Pro and the other to a γ-turn around Gly (Figure 6E). This oscillation between three structures results in average dihedral angles that are close to those expected for a type II β-turn and a somewhat lengthened Pro$^{\alpha}$CH$-$Gly$^{\alpha}$*NH* distance. The averaging over several structures is observed as a large distribution of ϕ,ψ angles in the Ramachandran plot for this tetrapeptide (Figure 4E).

6. Cyclo^{1,4}[Ac-Lys-Pro-Gly-Asp-NH$_2$] ($Tetra_{41}$). The short interproton ROESY distances from the $i + 2$ *NH* to the $i + 1$ $^{\alpha}$CH (2.29 Å) and to the $i + 3$ *NH* (2.80 Å) as well as the low temperature coefficient of the $i + 3$ *NH* (2.75 ppb/K) point to a type II β-turn conformation in this molecule. The constrained dynamics in both vacuum and DMSO exhibited a strong intramolecular hydrogen bond, the characteristic 10-member ring type II β-turn closure, between the Asp *NH* and the carbonyl of Lys. The Asp *NH* also showed a less populated hydrogen bond with the carbonyl of Pro. The $^{\epsilon}$*NH* of Lys was inside the ring during the entire simulation and showed some ability to H bond to the Lys carbonyl, consistent with its temperature coefficient (3.33 ppb/K). On the average, the backbone dihedral

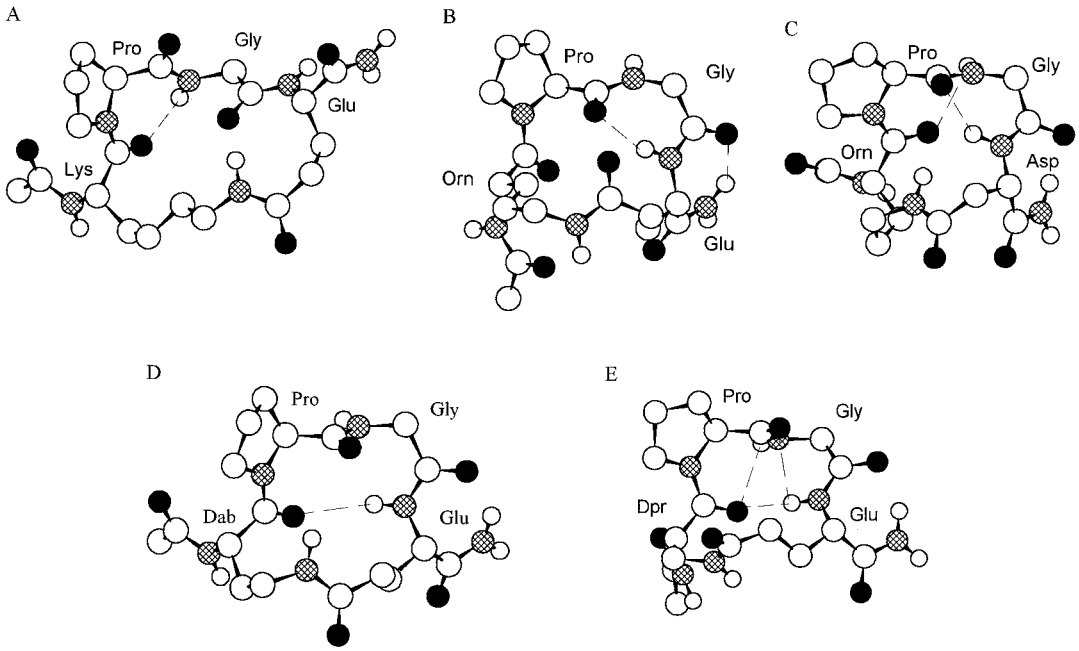

Figure 6. Averaged structures of cyclic model peptides in DMSO at 300 K: (A) $Tetra_{42}$; (B) $Tetra_{32}$; (C) $Tetra_{31}$; (D) $Tetra_{22}$; and (E) $Tetra_{12}$. The protons bound to carbon are not shown for clarity. The oxygens are displayed in black and nitrogens are stippled. The carbons and hydrogens are large and small open circles, respectively.

angles and the H-bond patterns from the simulations performed on this structure correspond to a type II β-turn.

7. Cyclo^{1,4}[Ac-Orn-Pro-Gly-Asp-NH$_2$] (Tetra$_{31}$). The relatively large (3.30 Å) ROESY distance observed between the *NH*'s of Gly and Asp excludes the possibility of a type II β-turn with Asp at the $i + 3$ position. Together with the low temperature coefficient exhibited by the Asp *NH* (2.65 ppb/K) this distance suggests the presence of a γ-turn-like ring around Gly. This conformational feature is observed in the dynamics simulations concurrently with a transient γ'-turn centered around Pro. The hydrogen bond between the Gly *NH* and the Orn carbonyl associated with the γ'-like ring repeatedly forms and breaks during the simulations which is consistent with the measured temperature coefficient of the Gly *NH* (3.45 ppb/K). A 10-membered H-bonded ring involving the Gly *NH*($i + 3$) and the Orn CO(i) is never observed in the simulations of this tetrapeptide. The average dihedral angles found in the simulations (Table 2) are consistent with two C_7 rings around Pro and Gly (Figure 6C).

8. Cyclo^{1,4}[Ac-Dab-Pro-Gly-Asp-NH$_2$] (Tetra$_{21}$). The simulations show that the $i + 3$ residue *NH* (Asp *NH*) forms H bonds to three different CO's belonging to the i (Dab), $i + 1$ (Pro), and $i + 3$ (Asp) residues. This extensive H bonding is consistent with the very low temperature coefficient determined for the Asp *NH* (−1.40 ppb/K). Although the average values of the backbone dihedral angles of the $i + 1$ and $i + 2$ residues are close to a type II β-turn conformation (Table 2), the 10-membered ring was the least populated in the MD simulation. The 7-membered ring involving the Pro CO appeared to be most stable. During the simulation a transient γ'-turn-like 7-membered ring closed by an H bond between the *NH* of Gly and the CO of Dab was also observed. Given the relatively high temperature coefficient of this *NH* (4.04 ppb/K) it is likely that this γ'-turn is not highly populated.

9. Cyclo^{1,4}[Ac-Dpr-Pro-Gly-Asp-NH$_2$] (Tetra$_{11}$). The MD simulations of this molecule exhibited a highly populated bifurcated hydrogen bond from the Asp *NH* to the α carbonyl of Dpr and to the β carbonyl of Asp. This is consistent with the very low temperature coefficient observed for this proton (−0.90 ppb/K). The Gly *NH* and the side chain *NH* both show temperature coefficients around 3 ppb/K. However, we note that all temperature coefficients for $Tetra_{11}$ are relatively low (Table 1). This molecule is the most constrained of the series and consequently its atoms experience less motion and perhaps less overall interaction with the solvent. The constrained dynamics indicated that the Gly *NH* and the lactam *NH* had a very low tendency to form an intramolecular H bond. The absence of such H bonding for the lactam *NH* is supported by six experimental ROESY derived distance constraints for this proton which result in its orientation to the outside of the cyclic portion of the molecule. The ROESY interproton distances from the Gly *NH* to the Pro $^{\alpha}$CH and to the Asp *NH*, 2.48 and 2.84 Å, respectively, and the 60 ps MD averaged dihedral angles (Table 2) concur with a type II β-turn conformation for this tetrapeptide.

10. Conformational Correlation. Previous investigations have attempted to correlate the effects of i to $i + 3$ and i to $i + 4$ lactamization on helix formation.[32] These studies concluded that both ring size and the orientation of the side chains involved in lactam formation influenced the stability of the helical segment under investigation. In particular an i to $i + 3$ lactam bridge with an 18-membered covalent ring was found to be helix destabilizing.[33] To our knowledge no previous study has attempted a systematic analysis of the effect of side chain lactamization on the stability of β-turns.

When trying to correlate the backbone conformation to the ring size in this series of closely related peptides, one is struck by the rich conformational diversity offered by what would be expected to be similar molecules. In the 16-membered cyclic

(32) (a) Felix, A. M.; Heimer, E. P.; Wang, C.-T.; Lambros, T. J.; Fournier, A.; Mowels, T. F.; Maines, S.; Campbell, R. M.; Wegrzynski, B. B.; Toome, V.; Fry, D. C.; Madison, V. S. *Int. J. Peptide Protein Res.* **1988**, *32*, 441−454. (b) Felix, A. M.; Wang, C.-T.; Campbell, R. M.; Toome, V.; Fry, D. C.; Madison, V. S. *Peptides: Chemistry and Biology, Proceedings of Twelfth American Peptide Symposium;* Smith, J. A.; Rivier, J. E., Eds.; ESCOM: Leiden,1992; pp 77−79. (c) Osapay, G.; Taylor, J. W. *J. Am. Chem. Soc.* **1990**, *112*, 6046−6051. (d) Osapay, G.; Gulyas, J.; Profit, A. A.; Gulyas, E. S.; Taylor, J. W. *Peptides: Chemistry and Biology, Proceedings of Twelfth American Peptide Symposium;* Smith, J. A., Rivier, J. E., Eds.; ESCOM: Leiden,1992; pp 239−240.

(33) Houston, M. E., Jr.; Gannon, C. L.; Kay, C. M.; Hodges, R. S. *J. Peptide Sci.* **1995**, *1*, 274−282.

peptides, $Tetra_{22}$ appears to form a stable type II β-turn while $Tetra_{31}$ assumes conformations involving γ-turn and γ'-turn-like C_7 rings. Similarly, in 17-membered cyclic peptides $Tetra_{41}$ seems to adopt a type II β-turn while the characteristic feature exhibited by $Tetra_{32}$ is that of a γ-turn-like C_7 ring. It was also found that cyclic peptides ($Tetra_{21}$ and $Tetra_{12}$) with 15-membered lactam rings exhibited entirely different structures. It was somewhat surprising that a β-turn-like structure was absent in the relatively flexible 18-membered lactam containing tetrapeptide ($Tetra_{42}$), while it was observed in $Tetra_{41}$. This finding together with the structural conclusions on the tetrapeptides containing smaller rings leads us to conclude that the exact conformation depends on the specific composition of the ring and does not correlate with the ring size. This conclusion could be further tested by preparing lactam rings in which the basic and acidic residues have been inverted in the primary sequence.

From the perspective of our analysis of the biologically active structure of the α-factor it is important to note that tridecapeptides containing lactams corresponding to $Tetra_{42}$, $Tetra_{32}$, $Tetra_{12}$, and $Tetra_{11}$ maintained the same preferred conformations as the model peptides (to be published elsewhere). Hence, it appears that one can control the architecture of a peptide by using the cyclized tetrapeptides discussed here as conformation fixing building blocks. This finding is important since many biologically active peptides contain β-turns and it is clear that cyclization through lactam bridges could result in the stabilization of this conformation. However, our findings indicate that the choice of the residues used for such lactamization is critical as different side chains can induce quite different structures.

5. Conclusions

In this paper we report a detailed conformational analysis of the major *trans* isomer of eight *i* to $i + 3$ side chain lactamized cyclic tetrapeptides containing a Pro-Gly dipeptide unit at the $i + 1$ and $i + 2$ positions and a systematic variation in the size of the constrained region (14- to 18-member rings). Our results show that, in contrast to what might be expected for a Pro-Gly sequence, several of these peptides exhibited preferences for the γ or γ' region of conformational space. Other peptides assumed a near-perfect type II β-turn and others were relatively flexible and underwent transitions between structures which were similar in energy. The Ramachandran maps (Figure 4) clearly indicate that for several structures the range of dihedral angles is highly limited while for others a greater range appears to be allowed implying additional flexibility. We believe that these plots incorporate all low-energy structures available to the Pro-Gly region of these molecules. In all peptides that were studied the $^{\alpha}$NH of the Gly is experimentally determined to be close to the $^{\alpha}$C*H* of Pro. Consequently, the ψ of Pro is always positive and all turns are far from a type I β-like conformation. We conclude that caution must be exercised while using such lactam constraints in the design of biologically active molecules with β-turns. Nevertheless, it appears that one can control the turn topology of a Pro-Gly peptide backbone by proper choice of the side chains used during lactamization.

Acknowledgment. The authors wish to thank Dr. Wei Yang for ROESY data on $Tetra_{42}$ and $Tetra_{32}$ and Dr. Leonardus van Gorkom for fruitful discussions. This work was supported by the NIH grants GM 22086 and GM 22087. The College of Staten Island NMR facility is funded by NSF grant BIR-9214560, The City University of New York, and The New York State Higher Education Advanced Technology Program.

Supporting Information Available: An additional 7 tables with comparisons between experimentally determined, and vacuum and DMSO simulated NOE derived interproton distances for seven peptides and a table comparing dihedral angles (ϕ) derived from coupling constants and the average values obtained from DMSO simulations for all the eight peptides (8 pages). See any current masthead page for ordering and Internet access instructions.

JA954217I